Time-Tagged Mission Execution Framework for Multi-Strip Imaging on a 6U CubeSat under COTS ADCS Constraints

Atif Mahmood, Ayman M Abadallah, Fatimah Kamal, Alzedany, XiXi Zhang
Interdisciplinary research center for Aviation and Space Exploration (Aerospace Engineering Department)
King Fahd University of Petroleum and Minerals (KFUPM)
Dhahran, KSA
atif.mahmood@kfupm.edu.sa, Aymanma@kfupm.edu.sa, (s202332550, s202465960)@kfupm.edu.sa

***Abstract*—This work presents an ADCS-driven agile imaging concept for enhancing the effective coverage of a 6U Earth-observation CubeSat through multi-strip imaging and attitude-based forward-motion compensation (FMC). Instead of relying on hardware modifications, the proposed method uses software-optimized attitude slews to dynamically reposition the line-of-sight during a single orbital pass, enabling the HyperScape-100 payload to capture multiple adjacent ground strips. A time-tagged mission execution sequence is developed, combining rapid retargeting maneuvers, payload triggering, and FMC-enabled pitch compensation to preserve image sharpness while maintaining modulation-transfer-function (MTF) performance. Simulation results show that agile slews on the order of 7–$8\ ^{\circ}$/s and attitude changes up to 15.8° can be reliably executed within 2-s maneuver windows. The required angular-rate and acceleration demands are shown to be achievable with commercially available COTS ADCS systems, confirming the feasibility of high-agility CubeSat imaging without custom hardware. The integrated approach increases effective coverage by more than a factor of three compared to static nadir imaging and demonstrates a scalable framework for future agile, software-defined EO missions leveraging existing spacecraft hardware.**

***Index Terms*—Agile Imaging, Multi-Strip Imaging, Mission Execution Plan, Slew Maneuver Planning, Satellite Control**

I. Introduction

Small Earth-observation (EO) satellites have expanded rapidly in capability, yet they remain fundamentally constrained by narrow swath widths and long revisit intervals compared to larger EO systems. Revisit time—the interval between repeat observations of a target region—is a critical performance parameter for monitoring dynamic phenomena such as vegetation change, dust events, flooding, and urban expansion. Large satellites overcome revisit limitations through wide-swath optics or multi-satellite constellations, such as Sentinel-2 achieving 5-day revisit at 10–20 m resolution [1], or commercial constellations like PlanetScope obtaining daily coverage using hundreds of small satellites [2]. In contrast, a single CubeSat-class spacecraft typically carries a compact imager with a swath of only tens of kilometers, resulting in revisit intervals of 10–30 days under nadir-only imaging [3]. Such long delays are inadequate for national monitoring needs in regions like Saudi Arabia, where timely observations support environmental programs and Vision 2030 objectives [4], [5].

With advancements in modern miniaturized attitude determination and control systems (ADCS), agile imaging has emerged as a promising strategy to overcome these revisit limitations without modifying payload hardware. By rapidly slewing the spacecraft's line-of-sight between adjacent ground tracks, a single small satellite can capture multiple strips within one orbital pass, effectively expanding its swath and reducing revisit time [6], [7]. Previous studies have explored off-nadir tasking, dynamic retargeting, and multi-strip imaging for large and agile platforms [8], [9], with recent scheduling approaches integrating image-quality constraints such as modulation transfer function (MTF) and motion blur into observation planning [10]. However, practical demonstrations on highly resource-limited 6U platforms remain scarce.

A key challenge in executing agile multi-strip imaging is preserving image sharpness during fast slews. Pushbroom imagers experience along-track smear due to ground-motion during exposure, restricting integration time to only a few tenths of a millisecond unless compensated. Forward motion compensation (FMC) techniques address this issue by adjusting either the spacecraft attitude or optical path to "freeze" the ground scene during integration. Spacecraft-level pitch motion compensation has been demonstrated on missions such as the Chinese ZH-1, which used attitude-driven FMC to significantly improve signal-to-noise ratio (SNR) without hardware changes [11]. Opto-mechanical FMC approaches, such as tilted secondary mirror systems, have shown even larger gains in exposure time [12]. These works highlight the potential of FMC to enhance performance of compact imagers, but they have not been integrated with agile retargeting on a 6U-class platform.

This paper presents a software-driven agile imaging concept for a 6U CubeSat carrying the HyperScape-100 hyperspectral imager. The method combines rapid ADCS-driven multi-strip retargeting with spacecraft-attitude-based forward motion compensation to expand effective swath coverage without modifying payload hardware. A case study over a large AOI in Saudi Arabia demonstrates that a sequence of closely timed slew–settle–image operations can be executed within the constraints of COTS ADCS systems while preserving image quality. Simulation results show that slews up to $\pm 6°$ at rates of up to 3°/s can be accommodated while satisfying stability, torque, and power limits, enabling more than a threefold increase in coverage during a single pass.

The main contribution of this work is the development of a unified, STK-optimized agile imaging framework that enables sequential multi-strip acquisition on a 6U CubeSat equipped with a COTS ADCS. Unlike previous studies that treat slewing, strip scheduling, and FMC independently, this work integrates all three elements into a practical mission execution workflow derived directly from high-fidelity STK orbit geometry. A complete time-tagged imaging sequence—validated within a constrained 2-s access window—is generated, demonstrating that six adjacent ground strips can be captured in only 16 s using rapid ADCS retargeting and attitude-based FMC. Detailed body-rate, acceleration, and torque requirements are derived and shown to be compatible with commercially available reaction-wheel-based ADCS systems, confirming that significant coverage expansion ($> 3\times$) can be achieved on a 6U platform without hardware modifications. This provides a reusable mission-planning methodology for small EO satellites seeking constellation-like coverage using software-defined agility alone.
Together, these contributions establish a practical and implementable mission-planning methodology for agile Earth-observation CubeSats, enabling significant coverage enhancement using only software-driven attitude agility. This generalized framework allows mission designers to systematically evaluate whether a new small EO satellite platform can support agile imaging, estimate the number of strips achievable per pass, and quantify potential improvements in coverage and revisit time, enabling rapid exploration and optimization during early mission design stages. In the following sections, we detail the system design and methodology, present the simulation results over the Saudi Arabia AOI, and discuss the operational considerations and potential generalization of this approach to other missions. Together, these contributions highlight a pathway for software-driven payload performance enhancement that can empower small satellites to meet demanding EO coverage requirements.

II. Problem Formulation

A. Background and Motivation

A 6U CubeSat carrying the HyperScape-100 hyperspectral payload has a swath width of only 20 km from an orbital altitude of 525 km. This narrow swath width causes large revisit intervals over the region of interest (ROI) of 2876.06 km × 20 km. Because of bus volume constraints, tight launch schedule, and the experimental nature of the payload, increasing the swath or re-procuring a new imager was not feasible. Hence, the mission objective is to reduce the effective revisit time by enabling agile attitude maneuvers using the ADCS subsystem, while staying within the available power limits. The imaging sequence progresses from the rightmost green strip to the leftmost yellow strip: Place/dam (1st), Place/vo (2nd), Place/ithr (3rd), Place/voc (4th), Place/aj (5th), and Place/dhma (6th), corresponding to the ground-strip mapping shown in Figures 1 and 2 and table I.

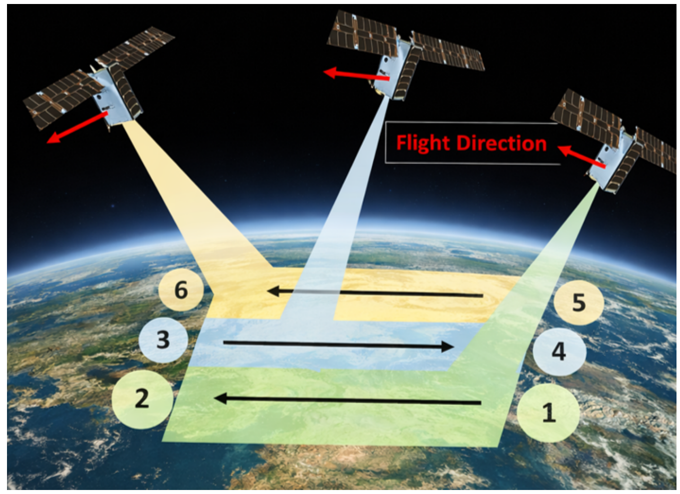

Fig. 1. Multiple Strip Coverage in one pass with agile Satellites for Smart Coverage

B. Imaging and Revisit Constraints

The HyperScape-100 payload provides a swath width of approximately 20 km, which is very narrow for large areas of interest (AOIs). Under nadir-only imaging, the CubeSat can observe only a single ground strip per orbital pass, leaving the majority of the AOI unobserved. Additionally, the orbital ground-track separation typically results in revisit intervals of 10–30 days, which is insufficient for applications requiring dynamic or time-sensitive monitoring. Pushbroom imaging further imposes strict along-track smear constraints during spacecraft slews, limiting the allowable exposure time unless forward-motion compensation (FMC) is applied. These combined limitations on swath, revisit time, and exposure duration motivate the need for a software-driven multi-strip agile imaging strategy integrated with attitude-based FMC. Access analysis indicates that the allowable maneuvering and stabilization interval between adjacent imaging strips is approximately 2 s, while the cumulative multi-strip imaging sequence during a single orbital pass spans approximately 16 s, as shown in Fig. 3.

C. Mission-Driven Optimization Formulation

The agile multi-strip imaging problem is formulated as a constrained mission-planning problem intended to maximize effective ground coverage during a single orbital pass while satisfying spacecraft operational constraints.

The decision vector is defined as

$$\mathbf{x} = [N_s, \theta_i, t_i, \omega_i] \tag{1}$$

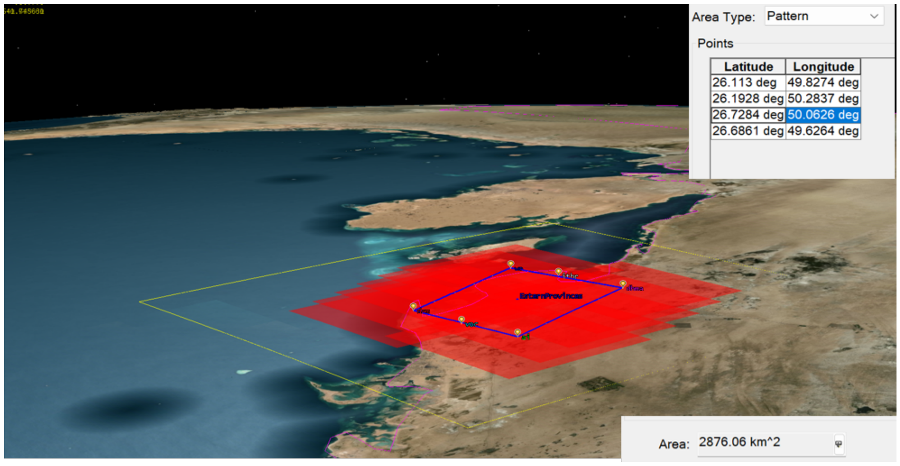

Fig. 2. Area of interest (AOI) in Saudi Arabia with planned multi-strip imaging pattern and overlaid adjacent ground tracks.

where N_s is the number of imaging strips, θ_i is the retargeting angle, t_i is the maneuver timing sequence, and ω_i is the spacecraft slew rate.

The optimization objective is expressed as

$$\max J = \alpha W_{eff} - \beta T_{revisit} \tag{2}$$

where

$$W_{eff} = N_s W_{payload} \tag{3}$$

subject to the operational constraints

$$P_{ADCS} + P_{payload} \leq P_{available} \tag{4}$$

$$|\omega_i| \leq \omega_{max} \tag{5}$$

$$\tau_i = I\alpha_i \leq \tau_{max} \tag{6}$$

$$t_{slew} + t_{settle} \leq t_{access} \tag{7}$$

$$\sigma_{LOS} \leq \sigma_{req} \tag{8}$$

where W_{eff} is the effective multi-strip swath width, $T_{revisit}$ is the effective revisit interval, σ_{LOS} is the line-of-sight pointing stability, and σ_{req} is the allowable imaging stability threshold. The imaging sequence is generated using STK-based orbital access analysis and sequential retargeting logic while satisfying ADCS maneuvering and image-quality constraints.

D. Modeling Assumptions

The present study considers a mission-level agile imaging feasibility analysis assuming rigid-body spacecraft dynamics under nominal low-Earth-orbit conditions. Power availability is assumed sufficient to support one agile multi-strip imaging sequence per orbital pass. The HyperScape-100 payload is assumed to support attitude-based forward-motion compensation (FMC) for image stabilization during agile retargeting maneuvers. The required FMC compensation is estimated from orbital ground-track motion and allowable image smear, yielding approximately $\pm 2^\circ$ correction along-track and across-track for the considered imaging geometry. The ADCS is assumed to execute sequential retargeting maneuvers while maintaining payload pointing stability within allowable imaging constraints. Access simulations indicate that 80 percent accumulated coverage is reached after roughly three months (Nov 2025–Feb 2026) as can be seen in figure 2. The maximum single-pass access window is limited to 2.0 seconds (figure 3), which bounds the duration available for each agile multi-strip imaging sequence. The present study represents a mission-level STK-based feasibility analysis assuming rigid-body spacecraft dynamics and nominal disturbance conditions.

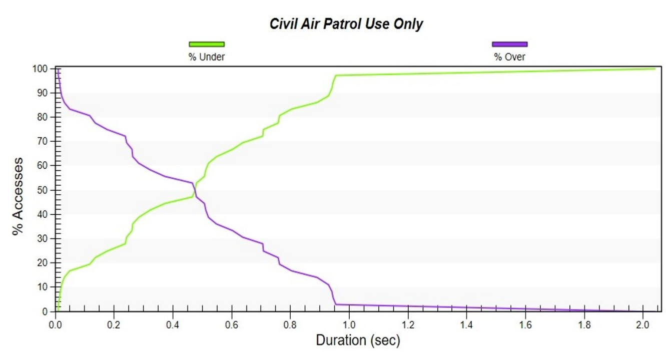

Fig. 3. Access duration across the AOI showing the maximum available 2 s imaging window.

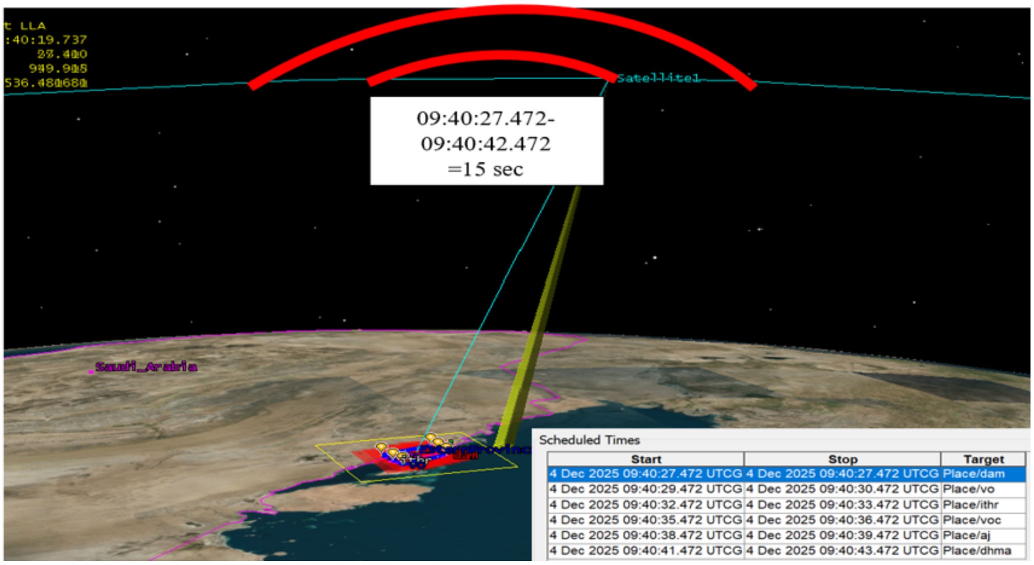

Fig. 4. Time-tagged multi-strip imaging sequence showing scheduled imaging and slewing intervals.

E. Orbit and Payload Model

The satellite is designed for a circular low-Earth orbit with a semi-major axis of 6,903 km (approximately 525 km altitude), a near-polar inclination of 96.77°, eccentricity 9×10^{-16}, argument of perigee $0°$, and RAAN $77.045°$. The detector captures up to 32 user-selectable VNIR spectral bands (with optional panchromatic band) using a 95-mm aperture, 580-mm focal-length optics and a 4096-pixel cross-track line-array CMOS sensor (5.5 μm pixel size, 12-bit depth). The payload mass is approximately 1.1–1.3 kg, with a power draw of 5–8 W in imaging mode and on-board storage of 128 GB, making it well suited for a 6U CubeSat bus.

- Total target area: $A_t = 2876.06$ km(figure 1)
- Swath width: $W = 20$ km
- Maximum access time to the area is 2 s (as shown in the figure 2)

III. Agile Imaging and FMC Methodology

The spacecraft agility requirements are directly derived from the time-constrained multi-strip imaging sequence. Assuming a symmetric maneuver profile, the required slew rate and angular acceleration are estimated as

$$\omega_{req} = \frac{2\Delta\theta}{t_{slew}} \tag{9}$$

$$\alpha_{req} = \frac{4\Delta\theta}{t_{slew}^2} \tag{10}$$

where $\Delta\theta$ is the required retargeting angle and t_{slew} is the allowable maneuver duration between adjacent imaging strips. Figure 4 illustrates the spacecraft LOS geometry during off-nadir agile imaging, defining the attitude transitions required for sequential multi-strip coverage. The agile imaging operation spans approximately 20 s (15 s imaging) and follows the sequence.

Pre-imaging $\rightarrow$ *Target-track* $\rightarrow$ *Imaging sequence* $\rightarrow$ *Nadir-hold*, with the corresponding time-tagged imaging windows shown in Fig. 5.

During *Pre-imaging*, the onboard computer (OBC) initializes the payload and configures the ADCS for the upcoming

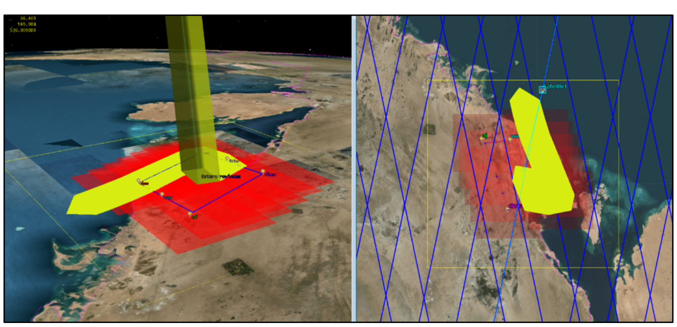

Fig. 5. Spacecraft retargeting sequence during agile multi-strip imaging.

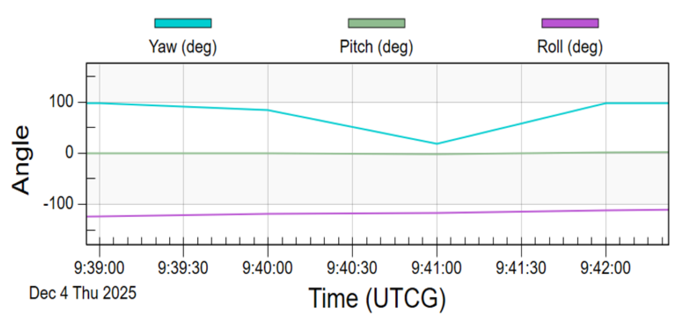

Fig. 6. Spacecraft body-axis attitude profiles during the agile multi-strip imaging sequence.

TABLE I
MANEUVERING AND RETARGETING PARAMETERS BETWEEN SEQUENTIAL IMAGING TARGETS.

Segment	**Dur. (s)**	$\Delta\psi$ (°)	$\Delta\theta$ (°)	$\Delta\phi$ (°)	$\overline{\omega}_\psi$ (°/s)	$\overline{\omega}_\phi$ (°/s)	ω (°/s)
Place/vo → Place/dam	2	10	0.3	3.3	5.0	1.7	5.4
Place/dam → Place/voc	2	8	0.3	2.7	4.0	1.3	4.2
Place/voc → Place/ithr	2	12	0.7	4.0	6.0	2.0	6.3
Place/ithr → Place/dhma	2	10	0.4	3.3	5.0	1.7	5.4
Place/dhma → Place/aj	2	15	0.4	5.0	7.5	2.5	7.9

maneuver, including camera power-up, timing alignment, and bus stabilization.

In *Target-track* mode, the ADCS executes pre-planned attitude maneuvers to align the payload line-of-sight with upcoming ground targets. The spacecraft may either slew or maintain a fixed inertial attitude depending on the imaging geometry.

The *Imaging sequence* consists of one or more back-to-back imaging windows, during which the payload actively acquires data while the OBC manages timing, buffering, and housekeeping telemetry.

Following completion of imaging, the spacecraft enters *Nadir-hold*, returning to nadir-pointing while the payload is powered down or placed in standby and data handling is prepared for downlink.

The full imaging sequence spans approximately 16 s and comprises alternating imaging and slewing intervals, as illustrated in Fig. 6.

Figures 6 and 7 illustrate the spacecraft attitude retargeting behavior during multi-strip imaging.

A. ADCS Hardware Requirements and Capabilities

Based on the required retargeting maneuvers, the attitude control system shall support average body-axis angular rates of at least 7.5 °/s (yaw), 2.5 °/s (roll), and 0.35 °/s (pitch) over a 2 s maneuver. This corresponds to a worst-case average three-axis slew rate of 7.9 °/s for a total attitude change of approximately 15.8° between consecutive observation points. The detailed values are provided in the table II. The attitude control system shall support retargeting maneuvers between consecutive observation points within 2 s. The required average body-axis angular rates derived from the maneuver set are 7.5 °/s (yaw), 2.5 °/s (roll), and 0.35 °/s (pitch), corresponding to a worst-case three-axis slew rate of 7.9 °/s. The design values adopted in this work are $\omega_{y,\max} = 10$ °/s, $\omega_{r,\max} = 4$ °/s, $\omega_{p,\max} = 1$ °/s, and a maximum three-axis slew rate of $\omega_{\text{slew},\max} = 10$ °/s. Assuming a trapezoidal rate profile, the required angular acceleration about the dominant axis is $\alpha_{\max} \approx$ 20–25 °/s^2, leading to an estimated worst-case control torque requirement of approximately 0.07–0.09 N·m and a corresponding wheel momentum requirement consistent with commercially available agile CubeSat ADCS systems.

B. Available COTS-ADCS Hardware

Simulation results indicate that the required maneuvering profiles are achievable using commercially available ADCS systems. Considering ADCS, EPS, and payload constraints, the proposed agile imaging operations are feasible on current 6U CubeSat platforms (Table III).

IV. DISCUSSION

Simulation results confirm that agile attitude maneuvers and forward-motion compensation enable significant coverage expansion for a 6U CubeSat hyperspectral imager without payload modification. **Feasibility of Multi-Strip Imaging** Tables II and III indicate that multi-strip imaging requires repeated slews of up to 15.8° within 2 s, corresponding to worst-case body rates of 7.9°/s. These rates fall within the performance envelope of modern COTS ADCS units, demonstrating the feasibility of agile multi-strip imaging on a 6U platform. However, the available maneuvering margin is limited, and larger off-nadir requirements may necessitate higher-torque reaction wheels or increased settle times. **FMC and Image Quality Considerations** Attitude-driven forward-motion compensation (FMC) is essential for maintaining image sharpness during aggressive slews. Without FMC, allowable exposure times are limited to sub-millisecond levels, significantly degrading SNR. By commanding a compensating pitch-rate profile, MTF compliance is maintained during each imaging window, consistent with demonstrated performance on higher-mass platforms such as ZH-1, and indicating that software-based FMC can extend exposure times on small satellites without optical-path modification. **Coverage and Revisit Improvement** The imaging sequence over the Saudi Arabia AOI (Figs. 4–6) demonstrates that six adjacent strips can be captured within approximately 16 s, yielding more than a threefold increase in swath width relative to the native 20 km footprint. When incorporated into long-term access simulations (Fig. 2), this expansion reduces effective revisit time for regions of national interest. Although a single 6U satellite cannot achieve constellation-level revisit, the proposed software-driven agility substantially narrows the gap. **Operational and System-Level Trade-offs** Despite its effectiveness, the agile imaging concept introduces nontrivial operational implications. Frequent large-angle slews increase reaction-wheel duty cycle, momentum buildup, and thermal load. Additional calibration may be required to maintain pointing accuracy during dynamic maneuvers. Power availability also limits the number of aggressive imaging sequences that can be executed per orbit. These system-level considerations must be incorporated into future flight software and mission planning.

V. CONCLUSION

This paper presented a software-driven agile imaging framework for a 6U CubeSat equipped with the HyperScape-100

TABLE II
DERIVED ADCS ANGULAR-RATE AND SLEW-RATE REQUIREMENTS

Parameter	**Formula**	**Derived Value**	**Requirement**	**Notes**
Max yaw rate	$\Delta\psi_{\max}/\Delta t$	$15°/2s = 7.5°/s$	$10°/s$	Dominant axis; margin applied
Max pitch rate	$\Delta\theta_{\max}/\Delta t$	$0.7°/2s = 0.35°/s$	$1°/s$	Small motions; rounded up
Max roll rate	$\Delta\phi_{\max}/\Delta t$	$5°/2s = 2.5°/s$	$4°/s$	With design margin
Worst-case rotation	$\sqrt{\Delta\psi^2 + \Delta\theta^2 + \Delta\phi^2}$	$15.8°$	—	Used to compute slew rate
Worst-case slew rate	$\Delta\alpha/\Delta t$	$15.8°/2s = 7.9°/s$	$10°/s$	Rate-limit bound
Required angular acceleration	ω_{peak}/t_a	$10.5°/s/0.5s \approx 21°/s^2$	20–25$°/s^2$	Trapezoidal 0.5–1–0.5 profile
Control torque	$I\alpha$	—	0.07–0.09 N·m	Assuming representative 6U inertia$I$
Wheel momentum	$I\omega_{\text{peak}}$	—	$H \geq 0.183I$ (N·m·s)	$\omega_{\text{peak}} \approx 0.183$ rad/s
Gyro measurement range	—	—	$\geq \pm 50°/s$	For fast slews

TABLE III
FEASIBILITY OF AGILE IMAGING USING AVAILABLE COTS ADCS SYSTEMS

Parameter	**Required**	**CubeSpace (CubeADCS Gen-2)**	**GomSpace (6U ADCS)**
Max body rate $\omega_{\max}$	$\geq 3\ °/s$	Achievable for CubeSpace.	10 °/s (published max slew rate).
Angular accel. limit $\alpha_{\max}$	$\geq 3\ °/s^2$	Wheel torque–limited (CubeWheel family).	Wheel torque–limited (Reaction Wheel family).
Pointing stability (rate) $\dot{\sigma}$	$\leq$ 0.005–0.02 °/s	Depends on sensor suite; CubeStar tracker gives 0.02–0.06° knowledge; stability controller-dependent.	Standard 6U config lists 1° pointing error; stability rate not specified; star tracker optional.
Pointing accuracy ε	$\leq$ 0.05–0.10 °	CubeStar Gen-2: 0.02–0.06° attitude knowledge (sensor); absolute depends on calibration.	Standard 6U bus: 1° pointing (baseline); higher precision with premium options or added sensors.
Settle margin per gap t_{settle}	1–1.5 s	Achievable with jerk-limited profiles and adequate wheel torque.	Achievable with jerk-limited profiles and adequate wheel torque.
Slew profile	Jerk-limited S-curve	Supported (closed-loop control).	Supported (closed-loop control).

payload, combining rapid ADCS retargeting with attitude-based forward-motion compensation (FMC) to expand effective swath coverage without payload hardware modification. Simulation results show that six adjacent ground strips can be imaged within a 16 s window, yielding more than a threefold coverage increase compared to nadir-only imaging. The resulting attitude-rate, acceleration, and torque requirements remain within the capabilities of commercially available COTS ADCS units, confirming the feasibility of agile multi-strip imaging on a resource-limited 6U platform. The results indicate that software-defined attitude agility with FMC can reduce effective revisit time and improve responsiveness for single-spacecraft Earth observation missions, enabling wide-area coverage without increased hardware complexity or constellation deployment. Future work will focus on higher-fidelity ADCS simulations, hardware-in-the-loop validation of FMC timing, and multi-orbit optimization under varying seasonal and geometric conditions.

REFERENCES

[1] M. Drusch et al., "Sentinel-2: ESA's optical high-resolution mission for GMES operational services," *Remote Sensing of Environment*, vol. 120, pp. 25–36, 2012.

[2] C. Cope et al., "PlanetScope imagery characterization and applications," *Remote Sensing*, vol. 11, no. 20, pp. 1–20, 2019.

[3] M. Mahdianpari et al., "A review of CubeSat-based Earth observation for monitoring applications," *Remote Sensing*, vol. 13, no. 15, pp. 1–28, 2021.

[4] J. Kabongo et al., "Satellite remote sensing for environmental monitoring in Saudi Arabia: Progress, challenges, and future directions," *Environmental Monitoring and Assessment*, vol. 194, no. 6, 2022.

[5] Saudi Vision 2030, "Environmental sustainability and geospatial initiatives," Vision 2030 Official Document, 2019.

[6] B. Kim, S. Park, and J. Choi, "Dynamic retargeting-based observation scheduling for agile imaging satellites," *Acta Astronautica*, vol. 128, pp. 98–112, 2016.

[7] Z. Jiang et al., "Multi-strip task scheduling for agile Earth observation satellites," *IEEE Trans. Aerospace and Electronic Systems*, vol. 56, no. 5, pp. 3762–3775, 2020.

[8] Y. Lu et al., "MTF-constrained multi-target observation planning for agile imaging satellites," *Remote Sensing*, vol. 16, 2024.

[9] Q. Liu, J. Fan, and H. Wang, "Attitude-based pitch motion compensation for pushbroom satellite imaging," *IEEE Trans. Geoscience and Remote Sensing*, vol. 54, no. 7, pp. 4482–4494, 2016.

[10] H. Zhang et al., "In-orbit performance of the ZH-1 hyperspectral satellite with pitch-compensation imaging," *ISPRS J. Photogrammetry and Remote Sensing*, vol. 158, pp. 79–92, 2019.

[11] M. Selimoglu et al., "Tilted secondary mirror mechanism for opto-mechanical forward-motion compensation," *Optical Engineering*, vol. 64, no. 1, pp. 013105, 2025.

[12] E. Baltsavias, "Image motion and pixel-smear analysis for airborne and spaceborne imaging systems," *ISPRS J. Photogrammetry and Remote Sensing*, 1999.

[13] X. Bai and D. Izzo, "Attitude control challenges for agile CubeSats: Analysis and design considerations," *Acta Astronautica*, vol. 152, pp. 561–574, 2018.

[14] B. Wie and D. Bailey, "Reaction wheel control system design for agile spacecraft," *Journal of Guidance, Control, and Dynamics*, vol. 31, no. 5, pp. 1273–1288, 2008.

[15] Z. Liu et al., "Scheduling dense imaging sequences for agile Earth observation satellites," *Aerospace Science and Technology*, vol. 114, pp. 106707, 2021.

[16] B. Xu et al., "Cooperative multi-satellite scheduling for Earth observation constellations," *Acta Astronautica*, vol. 165, pp. 49–61, 2019.